Solid State Ionics 18 & 19 (1986) 127-135
North-Holland, Amsterdam

EFFECTIVE POTENTIALS FROM LANGEVIN DYNAMIC SIMULATIONS OF FRAMEWORK SOLID ELECTROLYTES

R.O. ROSENBERG, Y. BOUGHALEB, A. NITZAN* and M.A. RATNER

Department of Chemistry and Materials Research Center, Northwestern University, Evanston, IL 60201 U.S.A.

Ionic motion in framework solid electrolytes constitutes a special sort of classical many-body problem. In such electrolytes, the conductivity is due to the motion of interacting mobile ions modulated by the presence of an essentially immobile framework sublattice. Here, a one-dimensional model of interacting particles, governed by Langevin's equations of motion in a sinusoidal potential, is used to calculate particle distribution functions and effective potentials. The effective potential $V_{eff}(x)$, is then defined through the density distribution, $\rho(x)$, $\rho(x) \propto e^{-\beta V_{eff}(x)}$ where $\beta = 1/kT$. The Langevin dynamics simulation is used to calculate $\rho(x)$, which in turn gives $V_{eff}(x)$. The dc conductivity and the other distribution functions can be used to investigate commensurability effects, pinning effects, and screening effects. Comparisons can then be made between correct numerical many-body results and various analytical approximations.

In solid framework electrolytes some of the constituent ionic species exhibit conductivity of the same order of magnitude as that of liquid electrolytes.[4] Potassium hollandite is one such conductor in which the mobile potassium ions move through an ionic framework dominated by octahedral sites.[2] In this type of conductor, the ionic sublattice is rigid and one can discuss theoretical models that treat the dynamics of the mobile ions as independent of dynamics of the sublattice. Further simplifications can be employed concerning mobile ion-ion interactions[3-5] and mobile ion-sublattice interactions.[6] Many models have been proposed but even with such simplifications, ionic transport in solid framework electrolytes is a difficult many-body problem. Analytical treatments of the problem go from simple lattice gas and hopping models[7-15] to dynamical treatments including continued fraction solutions of the Fokker-Planck equation.[16-18] Numerical solutions, which treat the many-body dynamics exactly, include both molecular[19-22] and Langevin dynamics.[23-28] This paper uses Langevin dynamics to examine the properties of these superionic conductors. This model assumes that the rigid sublattice interacts with the mobile ions only through a static potential due to the sublattice equilbrium configuration and a dissipative mechanism that exerts both a viscous drag and a random force to maintain thermal equilibrium. In the high friction limit, Dieterich[29-32] has shown that the dynamics of the mobile ions become even simpler and

*Permanent Address: Department of Chemistry, Tel-Aviv University, Tel-Aviv, Israel

0 167-2738/86/$ 03.50

one can relate the DC conductivity to an effective potential which is defined in terms of the single particle density function. In turn, experimentalists can obtain the single particle density function from diffuse X-ray scattering experiments.[33-35]

It is the purpose of this paper to see if such a relation can hold for a broader range of frictions and interaction potentials: for what mobile ion densities, temperatures, frictions, and particle interactions can the many particle dynamics be represented by the single particle dynamics in the effective potential. The picture is obviously limited and is not expected to apply in all circumstances, however the concept of effective potential greatly simplifies the many-body problem so that a broader range of superionic conductors may be studied and ionic transport more fully understood. It is therefore worthwhile to push this concept as far as possible and to explore its limits. We present here such effective single-particle potentials, derived from full Langevin simulations, for a series of physical situations (differing frictions, densities, potentials, and temperatures) in a one-dimensional model.

We consider here a one-dimensional model of interacting particles, governed by Langevin's equations of motion[36-38] in a sinusoidal potential. The Langevin equation of motion for a single particle is

$$m\ddot{x}_i = -m\gamma\dot{x}_i - \frac{\partial}{\partial x_i} V_{TOT}(\{x\}) + R_i(t) \qquad (1)$$

where m is the mass of the particle, γ is the friction coefficient, $V_{TOT}(\{x\})$ is the total static potential and $R_i(t)$ is the random force, assumed to be gaussian white noise. The random force and the friction coefficient are related by the second fluctuation dissipation theorem[39]:

$$\langle R_i(t)\, R_j(o)\rangle = 2mkT\gamma\delta(t)\delta_{ij} \qquad (2)$$

where k is Boltzmann's constant and T is the temperature. There are four interesting parameters to vary: the particle concentration C, the friction coefficient, the temperature, and the static potential.

The total static potential for ionic motion in a system with N mobile ions contains both one- and two-body terms:

$$V_N(\{x\}) = \sum_i V_1(x_i) + \sum_{i>j} V_2(x_i - x_j) \qquad (3)$$

$V_1(x)$ is the sinusoidal potential due to the equilibrium configuration of the cage potential of the sublattice,

$$V_1(x) = \frac{A}{2}\left[\cos\left(\frac{2\pi x}{a}\right) + 1\right] \qquad (4)$$

where A is the barrier height, a is the distance between wells, and the well-bottom frequency is $\omega_0 = [2\pi^2 A/ma^2]^{1/2}$. The mobile ion interactions are assumed to be the sum of pair interactions, $V_2(x_i - x_j)$ such as the coulomb potential,

$$V_2(x_i - x_j) = q^2/|x_i - x_j| \qquad (5)$$

where q is an effective charge. Other potentials that we consider are a short range potential[40,41]

$$V_2(x) = B\left[\left(\frac{b}{x}\right)^2 - 1/9\right], \quad x \leq 3b;$$
$$V_2(x) = 0, \quad x > 3b \qquad (6)$$

with a cutoff at x = 3b, and the Frenkel-Kontorova interaction[6,16]

$$V_2(x_i - x_j) = \alpha(x_i - x_j - b)^2 \quad \delta_{i,j\pm 1} \qquad (7)$$

which assumes harmonic interactions only between nearest neighbors. These three different potentials will serve to investigate how the effective potential varies with the type of interaction chosen for the mobile ions.

The mobile ion effective potential $V_{eff}(x)$ is then defined through the single particle distribution function,

$$\rho(x) \equiv z\, e^{-\beta V_{eff}(x)} \qquad (8)$$

where $\beta = 1/k_B T$ and z is a normalization constant. The Langevin dynamics simulation provides trajectories to calculate $\rho(x)$ and thus obtain $V_{eff}(x)$. In the high friction limit, the DC conductivity of the system can be expressed in terms of the effective potential

$$\sigma = \rho_0 D_0 \beta q^2 [\frac{1}{a} \int_0^a dx\, e^{\beta V_{eff}(x)} \times \frac{1}{a} \int_0^a dx\, e^{-\beta V_{eff}(x)}]^{-1} \quad (9)$$

where ρ_0 is the average density and D_0 is the bare ion diffusion coefficient. Thus given the density, $\rho(x)$, one can obtain (in the Smoluchowski limit) the DC conductivity σ. This formula is exact for noninteracting particles. It is the purpose of this paper to see for what range of frictions, densities, and interaction potentials one can relate the many particle dynamics to the single particle dynamics in an effective potential, and to study the systematics and behavior of this effective potential.

The height and well frequency of the effective potential give a good indication of the dynamics of the system. For commensurate densities, where the preferred spacing of the ions due to their interaction potential, V_2, is commensurate with the bare sinusoidal potential, V_1, (V_1 and V_2 can assume their minimum energies simultaneously) we expect the effective potential to have a higher barrier height than the bare sinusoidal potential. In this commensurate case, the two parts of the potential reinforce each other, requiring an escaping particle to gain that much more energy before exiting a well. Since the effective potential barrier height is increased compared to A, we expect the effective well curvature to be higher, and this should be reflected in the conductivity peak for the single-particle effective dynamics. For the incommensurate case, in which the interaction potential favors an ion spacing incommensurate with the bare lattice spacing, the effective potential barrier may be reduced. Here the potentials V_1 and V_2 compete, since they cannot assume their minima simultaneously for any configuration of ions. Thus the equilbirium ionic configuration requires ions to sit away from their sinusoidal potential well minima in order to decrease their total interaction energy. The resulting ion configuration can best be seen by looking at the pair correlation function, which is defined in terms of the two particle and single particle probability densities:

$$g(x,x') = \rho^2(x,x')/\rho(x)\rho(x') \quad (10)$$

$g(x,x')$ is the conditional probability of an ion being at x' given that there is an ion at x. Let us call the ion at position x the test ion. For an inhomogeneous system, we consider only two pair correlation functions, one where the test ion is at the bottom of the well and another where the test ion is between wells at the barrier top. These two pair correlation functions will indicate the importance of the sinusoidal potential; if it is important the top and bottom pair correlation functions will be quite different, if the effect of sinusoidal potential is small, they will be similar. The pair correlation function will also indicate how the ions, in an equilibrium average, space themselves among the wells. From equation (9), those densities resulting in ions with equilibrium positions near the barrier tops are indicative of an increase in the DC conductivity.

The frequency-dependent conductivity is related to the frequency-dependent diffusion coefficient by the Nernst-Einstein relation:

$$\sigma(\omega) = Cq^2 \beta D(\omega) \quad (11)$$

Here the frequency dependent diffusion coefficient is found by the Green-Kubo relation

involving the Fourier transform of the velocity-velocity time correlation function:

$$D(\omega) = \mathrm{Re}\{\int_0^\infty e^{i\omega t} \langle v(t)\ v(0)\rangle\ dt\} \qquad (12)$$

where $\langle\ldots\rangle$ denotes a canonical ensemble average. Either the tracer or bulk diffusion coefficient can be calculated

$$D_{Tr}(\omega) = \mathrm{Re}\{\frac{1}{N}\sum_{i=1}^{N}\int_0^\infty e^{i\omega t}\langle v_i(t)\ v_i(0)\rangle dt\} \qquad (13)$$

$$D_{Bu}(\omega) = \mathrm{Re}\{\frac{1}{N}\sum_{i=1}^{N}\sum_{j=1}^{N}\int_0^\infty e^{i\omega t}\langle v_i(t)\ v_j(0)\rangle dt\} \qquad (14)$$

where N is the number of particles. In order to determine convergence, we compare $D_{Bu}(0)$ to the DC conductivity obtained from the slope of the mean square displacement:

$$D_{Bu} = \frac{1}{N}\sum_{i,j}^{N}\lim_{t\to\infty}\langle(x_i(t) - x_j(0))^2\rangle/2t \qquad (15)$$

Note that in one dimension $\sigma(\omega)$ (eq. (11)) is related to the total current in the chain and not to the current per unit cross-sectional area.

RESULTS

The parameters of the system were those used by Jacobson, et al.,[31] to simulate potassium hollandite and silver iodide. The lattice spacing was taken to be 3.1 Å, the well height to be .1 eV and the ion mass was that of silver. The other parameters, friction, temperature, and density, were varied for each simulation. We define the concentration C as the number of ions per site. Our high friction calculations were done with $\gamma = 1.6\ \omega_0$ where ω_0 is the well bottom frequency. In this regime previous numerical work[31] showed that the Langevin dynamics for a system of coulomb particles agreed fairly well with Dieterich's Smoluchowski result, Eq. (9). Low friction was represented by $\gamma = 0.08\omega_0$. The temperature was taken to be A/3 for the short range interaction potential and A/2 for the coulomb and Frenkel-Kontorova systems. For each potential, commensurate and incommensurate densities were used. For the short range interaction potential, the ion behavior is very liquid-like. The preferred ion spacing was taken to be the position of the first maximum in the pair correlation function for the system in the absence of sinusoidal potential. Following Bunde[40] the commensurate and incommensurate densities and radii are taken as C = 0.8, 1.6 and b = .5a, .25a, respectively. For the FK potential C = 0.5 and 0.67 for commensurate and incommensurate densities, while for coulomb interactions these values are 0.5 and 0.75. The FK force constant α is fixed by

$$\alpha = \frac{2\pi^2\ \kappa^{-1}\ kT}{b^2},\quad \kappa^{-1} = 2,\ b = C\cdot a$$

which is weak enough so that ions can almost pass through each other. For the coulomb system we use an effective charge of .6 times the charge of an electron. This implies that for a pair of ions in the system with C = 0.5, at the equilibrium pair distance (in the absence of the sinusoidal potential) the potential energy per particle is about ten times the barrier height.

In Fig. 1 we show the pair correlation functions g(x,x') for the short range interaction and coulomb potentials for both the commensurate and incommensurate cases. For both potentials, the incommensurate pair correlation functions are similar while for commensurate densities the functions are very different. Thus the sinusoidal potential is relatively unimportant for the incommensurate cases with strong repulsive interactions, and the ions act like a homogeneous liquid, so that $g(x,x') \cong g(x-x')$. In the commensurate case the periodic potential is very important. The sharp peak in the "well top" pair correlation function appears because the test ion interaction with

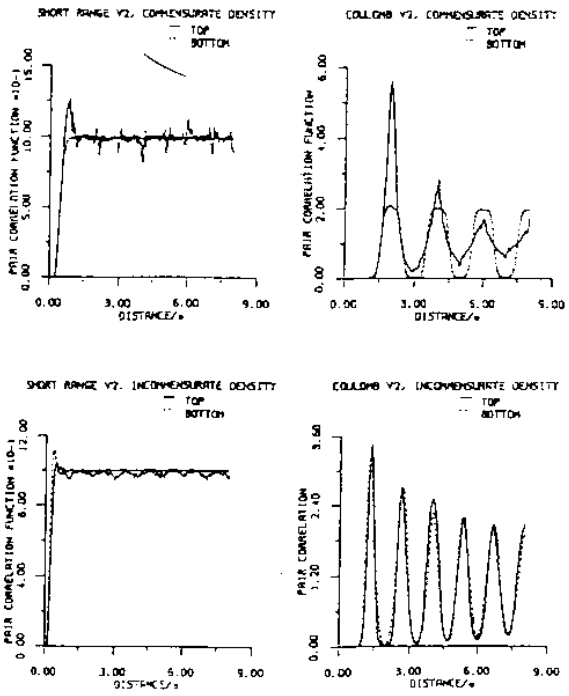

FIGURE 1

Pair correlation functions g(x,x') for the short range interaction (A = 3kT, T = 387.33 K and C = 0.8, 1.6 and b = a/2, a/4 for commensurate and incommensurate densities, respectively) and coulomb interaction (q = .6, kT = 581 K and C = 0.5, 0.75 for commensurate and incommensurate densities, respectively). Here m = 1.77 x 10^{-22} gm, A = .1 eV and a = 3.1 Å.

the first neighboring ion is so strong it drives the ion to the opposite side of the well, pinning it near the top of the well. The neighboring ion's mobility is reduced and correspondingly its probability of being found in this position greatly increased resulting in the large peak in the pair correlation function. Comparing the pair correlation function of the two potentials, we see that the short range interaction is much more liquid-like; it decays to unity after one site, while the coulomb potential is probably still correlated even after dozens of sites. The coulomb pair correlations have important implications for dc conductivity. For the commensurate density, the ions sit at the well minima. For the incommensurate case, of the six peaks representing the six nearest neighbor ions, four of these ions have equilibrium positions away from the sinusoidal well minima. These arrangements of the ions indicate that DC conductivity for the incommensurate density will be greater than that for the commensurate case.

In Fig. 2 we show the effective potentials. In the commensurate cases the barrier height stays the same or increases, while in the incommensurate case the barrier height is greatly reduced. One can see also that the curvature of the well bottom changes drastically as the effective barrier height changes; this should be reflected in a red shifted peak frequency in the single particle conductivity spectrum. When comparing the two potentials, the effective potential is much more sensitive to the density in the coulomb system than in

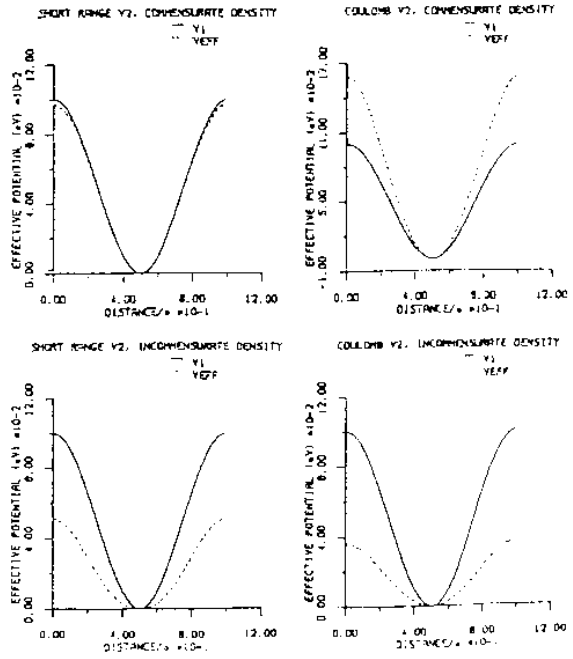

FIGURE 2

Effective potentials, $V_{eff}(x)$, for the short range and coulomb interactions. Same parameters as Figure 1.

TABLE 1

DC conductivities for various potentials, densities, and frictions. Systems: SR = short range, FK = Frenkel-Kontorova, CO = coulomb. Density: C = commensurate density, I = incommensurate density; Friction: H = High friction, L = low friction.

System	Density	Friction	σ^a	σ^b	$\sigma(0)^c$	$\sigma(0)^d$	$\sigma_{Smol}{}^e$
SR	C	H	.24	.27	.29	.27	.32
		L	1.20	1.8	.99	1.8	6.5
	I	H	1.0	1.1	1.1	1.1	1.2
		L	10.0	9.2	12.0	9.7	24.0
FK	C	H	.30	.40	.38	.41	.52
		L	.89	2.4	.74	2.4	10.0
	I	H	1.2	1.3	1.3	1.3	1.3
		L	9.0	13	8.8	14	26.0
CO	C	H	.13	.28	.19	.28	.39
		L	.24	1.8	.26	1.8	7.9
	I	H	1.4	1.5	1.4	1.5	1.6
		L	19.0	20.0	20.0	21.0	32.0

$x10^{-3}$ (mho/cm)

a. From mean square displacement Eq (15), many particle result.
b. From mean square displacement Eq. (15), single particle in effective potential result.
c. From zero frequency conductivity, Eq. (14), many particle result.
d. From zero frequency conductivity, Eq. (14), single particle in effective potential result.
e. From Smoluchowski value (Eq. (9)).

short range interaction system. This is because the coulomb system has very strong ion-ion interactions. Such strong interactions can more effectively diminish or reinforce the bare sinusoidal potential.

Now consider the DC conductivity. In Table 1, the values of the DC conductivity are given for all three systems: short range interaction (SR), Frenkel-Kontorova (FK), and Coulomb (CO). For each system we report values for the commensurate (C) and incommensurate (I) densities, and for high (H) and low (L) frictions. In each case four values are listed. Those values taken from the mean square displacement are denoted by σ and those taken from the integral of the velocity autocorrelation function are denoted by $\sigma(0)$. The primes indicate the single particle results in the effective potential. A fifth value is given using Eq. (9). All values are given in units of $(ohm*cm)^{-1}$. In the high friction limit, we can see that the conductivities are close to their Smoluchowski values. However comparison of σ_D and $\sigma(0)$ reflects the numerical difficulty in evaluating the latter. Despite these difficulties, one can see that for the low friction values, the short range potential yields much better agreement between the many body and single particle DC conductivities than for the other two potentials.

In Figs.3 and 4 we show the frequency dependent bulk conductivity for the short range and

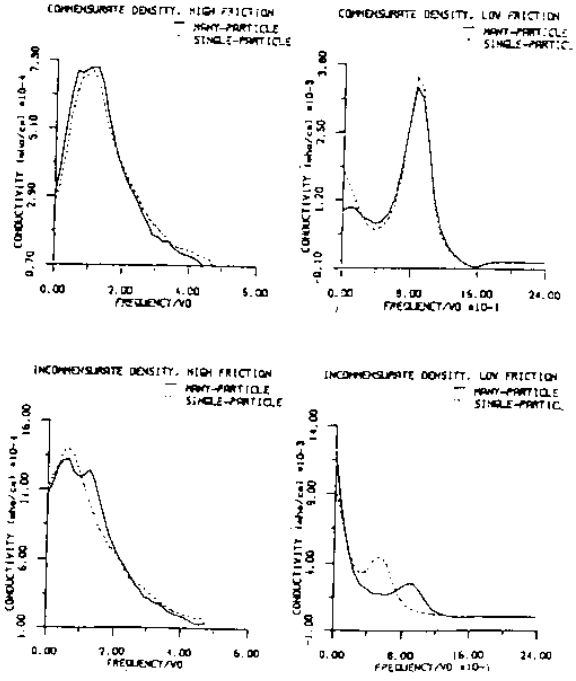

FIGURE 3
Frequency dependent conductivity for the short range interaction. Conductivities for commensurate and incommensurate densities and for high and low frictions. $\gamma = 6.82 \times 10^{12}$Hz, 0.341×10^{12} Hz for high and low friction, respectively.

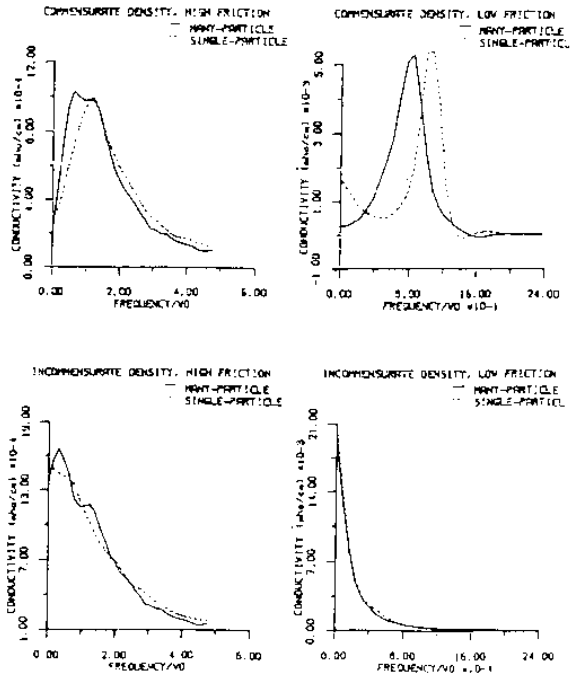

FIGURE 4
Frequency dependent conductivity for the coulomb interaction; parameters as in Figures 1,3.

coulomb systems, respectively. On each plot two curves are shown. The solid line is for the full many-body system calculated from eqs.(11,12), the second is the single particle dynamics calculated from eq.(12) in the many particle effective potential defined by eq.(8). In Fig. 3 the results for the short range potential are shown. In the high friction case we obtain very good agreement between the many and single particle dynamics. The interesting results are for the low friction regime. Here Dieterich's formula eq.(9) does not hold and it is of interest to see if the single particle dynamics still can duplicate the many particle dynamics. In the commensurate case there is good agreement for all frequencies. For the incommensurate case we see that both curves show both Drude and oscillatory behavior, but that the oscillator peak comes at a lower frequency using the effective potentials; the effective barrier height is reduced, thus the well bottom curvature is lowered, lowering the single particle frequency of motion. For the coulomb system (Fig. 4), we again see very good agreement for the high friction results. For the low friction regime in the commensurate case the correspondence is poor. The many-particle results show only oscillatory behavior, but the single-particle dynamics show an oscillatory peak at a higher frequency and also Drude behavior. For the incommensurate case both curves show only Drude behavior and hence very good agreement.

Results were also obtained for the Frenkel-Kontorova model. They were very similar to the coulomb system except for the low friction incommensurate case. For this system the agreement with single-particle results was poor; for the single-particle conductivity, a much larger Drude peak and an oscillatory peak were present where the many-particle conductivity had none. These results, although not

extensive, indicate that the low friction Langevin results in the effective potential obtain fair agreement with the many-particle results for both ranges of potential.

REMARKS

Although these studies show several interesting physical phenomena, including commensurability effects, strong ordering, liquid-like transport, etc., the feature of greatest interest is the effective single-particle potential, which is defined by eq.(8), and has been invoked previously to help in the interpretation of diffraction data and in the relationship of structure to conductivity. The definition (8) is based on the equilibrium distribution and one would expect its utility to diminish in situations where nonequilibrium dynamics plays an important role (i.e., low friction). Nevertheless, we find that the effective potential, as derived from Langevin simulations for a series of potentials, densities, temperatures, and frictions does provide a good qualitative, and in most cases even a good quantitative, estimate of the true conductivity, both at dc and even over the entire frequency range. The agreement between the results of the full, many-particle simulation and the motion in the effective potential is best for the smooth, long-range coulomb interaction. For this interaction in the low friction commensurate density situation the agreement is poorer: weakly-damped dynamical correlations will lower the effective frequency, widen the vibrational line, and much decrease the dc conductivity compared to the effective single-particle dynamics. For short-range potentials, the overall agreement is slightly worse, and becomes quite poor for incommensurate density at low friction.

The very interesting theoretical question of just how to define $V_{eff}(x)$ without the simulation (or diffraction data) has been considered several times. On the basis of our results here, it is clear that these effective potentials are of real value and interest, and that their derivation using some valid and accurate decoupling approximation remains an objective of real importance.

ACKNOWLEDGMENTS

We are grateful to the ARO, AFOSR, and to the NSF-MRC program for support, the latter through the Northwestern MRL (grant number DMR-82-16972). We also thank A. Pechenik and S. Druger for helpful remarks.

REFERENCES

1. (a) M. Salamon, Physics of Superionic Conductors (Springer, Berlin, 1979).

   (b) P. Vashishta, J. Mundy and G. Shenoy, Eds. Fast-Ion Transport in Solids (North-Holland, Amsterdam, 1979).

   (c) G. C. Farrington and J. Bates, Eds. Fast-Ion Transport in Solids (North-Holland, Amsterdam, 1981).

   (d) G. Mahan in Superionic Conductors, ed. G. Mahan and W. Roth (Plenum, New York, 1976).

2. T. Geisel, Sol. St. Comm. 322 (1979) 739.

3. H. U. Beyeler, Phys. Rev. Lett. 37 (1976) 1557.

4. H. U. Beyeler and C. Schuler, Sol. St. Ionics 1 (1980) 77.

5. W. Dieterich, P. Fulde, and I. Peschel, Adv. Phys. 29 (1980) 527.

6. B. Bruesch, S. Strassler, and H. Zeller, Phys. Stat. Sol. A31 (1975) 217.

7. P. M. Richards in Fast-Ion Transport in Solids, ed. P. Vashishta, J. Mundy and G. Shenoy (North-Holland, Amsterdam, 1970).

8. J. B. Boyce and B. A. Huberman, Phys. Rep. 51 (1979) 189.

9. J. C. Kimball and L. W. Adams, Phys. Rev. B18 (1978) 5351.

10. J. M. Girvin and G. D. Mahan, Sol. St. Comm. 23 (1977) 629.

11. G. D. Mahan, Phys. Rev. B14 (1976) 780.

12. P. N. Richards, Phys. Rev. B16 (1977) 1393.

13. K. Funke, Prog. Solid State Chem. 11 (9176) 345.

14. I. Bernasconi, S. Alexander and R. Orbach, Phys. Rev. Lett. 41 (1976) 185.

15. Y. Boughaleb and J. F. Gouyet, Sol. St. Ionics 9/10 (1983) 1401.

16. T. Geisel, Phys. Rev. B20 (1979) 4294.

17. T. Geisel, Sol. St. Comm. 24 (1977) 155.

18. P. Fulde, L. Pietronero, W. P. Schneider and S. Strassler, Phys. Rev. Lett. 35 (1975) 1776.

19. P. Vashishta and A. Rahman, Phys. Rev. Lett. 40 (1978) 1337.

20. T. Schneider and B. Stoll, Phys. Rev. B22 (1980) 5317.

21. S. W. Leeuw and J. W. Perram in Fast-Ion Transport in Solids, ed. P. Vashishta, J. Mundy and G. Shenoy (North-Holland, Amsterdam, 1979).

22. M. L. Wolf and C. R. A. Catlow, J. Phys. C: Solid State Phys. 17 (1984) 635.

23. S. H. Jacobson, A. Nitzan and M. A. Ratner, J. Chem. Phys. 73 (1980) 3712.

24. S. H. Jacobson, M. A. Ratner and A. Nitzan, Phys. Rev. B23 (1981) 1580.

25. S. H. Jacobson and M. A. Ratner, Sol. St. Ionics 5 (1981) 129.

26. S. H. Jacobson, A. Nitzan, and M. A. Ratner, Sol. St. Ionics 5 (1981) 125.

27. S. H. Jacobson, M. A. Ratner, and A. Nitzan, J. Chem. Phys. 77 (1982) 5752.

28. S. H. Jacobson, M. A. Ratner, and A. Nitzan, J. Chem. Phys. 78 (1983) 4154.

29. W. Dieterich, I. Peschel, and W. P. Schneider, Z. Phys. B27 (1977) 177.

30. A. R. Bishop, W. Dieterich, and I. Peschel, Z. Phys. B33 (1979) 187.

31. W. Dieterich, I. Geisel, and I. Peschel, Z. Phys. B29 (1978) 5.

32. S. E. Trullinger, M. C. Miller, R. A. Guyer A. R. Bishop, F. Palmer, and J. A. Krumhansl, Phys. Rev. Lett 40 (1978) 206.

33. H. Schultz and U. H. Zucker, Sol. St. Ionics 5 (1981) 41.

34. R. J. Cava, Sol. St. Ionics 5 (1981) 47.

35. B. H. Grier, S. M. Shapiro, and R. J. Cava, Phys. Rev. B24 (1984) 3810.

36. S. A. Adelman, J. Chem. Phys. 74 (1981) 4646.

37. S. A. Adelman and J. Doll, J. Chem. Phys. 64 (1976) 2375.

38. A. Nitzan, M. Shugard, and J. Tully, J. Chem. Phys. 69 (1978) 2525.

39. R. Kubo, Rep. Prog. Phys. 29 (1966) 225.

40. A. Bunde, Z. Phys. B44 (1981) 225.

41. A. Bunde, and W. Dieterich, Sol. St. Comm. 37 (1981) 229.

42. J. L. Tully, G. H. Gilmer, and M. Shugard, J. Chem. Phys. 71 (1979) 1630.